Mobility Parameter Tuning for Device Simulation

Tibor Grasser
Institute for Microelectronics
TU Vienna
A-1040 Vienna, Austria
grasser@iue.tuwien.ac.at

Siegfried Selberherr
Institute for Microelectronics
TU Vienna
A-1040 Vienna, Austria
selberherr@iue.tuwien.ac.at

Katsumi Tsuneno
Hitachi, Ltd., 16-3, Shinmachi
6-Chome, Ome-shi, Tokyo
198-8512, Japan
tuneno@cm.ddc.hitachi.co.jp

Hiroo Masuda
Hitachi, Ltd., 16-3, Shinmachi
6-Chome, Ome-shi, Tokyo
198-8512, Japan
masuda@cm.ddc.hitachi.co.jp

Abstract

We present our results of tuning mobility model parameters with an automated calibration framework. Observing a state-of-the-art 0.25 μm *CMOS process, several measurements for different gate lengths (0.25–4.0* μm*) were made. To eliminate the statistical variations typical to sub-micron devices, measurements for several chips on the the same wafer were made to chose an average sample. Carrying out simulations with the resulting parameter set, an error smaller than 2.4% for both the long-channel and the short-channel device can be observed.*

1. Introduction

The backbone of todays engineering work is formed by the meanwhile highly effective process and device simulators (e.g., [2], [3], [4]) which are generally available. The accuracy of these simulators is known to be very good for many engineering purposes. Nevertheless, many models implemented in these simulators have a limited range of accuracy due to the complex nature of the underlying physics. The parameters of these models are normally not so well known, displayed by the strong deviation of the values found in literature. To achieve high accuracy for a distinct process essential parameters need to be calibrated.

In our application the process was simulated using TSUPREM4 and for the device we used MINIMOS. We focused on the calibration of the MINIMOS6 mobility model, a description of which can be found in [5]:

$$\mu_n^{LIS} = \frac{\mu_n^{ref} + (\mu_n^{LI} - \mu_n^{ref}) \cdot (1 - F(y))}{1 + F(y) \cdot \left(\dfrac{S_n}{S_n^{ref}}\right)^{\gamma_n}}$$

$$\mu_n^{LISF} = \frac{2 \cdot \mu_n^{LIS}}{1 + \left[1 + \left(\dfrac{2 \cdot \mu_n^{LIS} \cdot F_n}{v_n^{sat}}\right)^{\beta_n}\right]^{\frac{1}{\beta_n}}}$$

$$F(y) = \frac{2 \cdot \exp\left[-\left(\dfrac{y}{y^{ref}}\right)^2\right]}{1 + \exp\left[-2 \cdot \left(\dfrac{y}{y^{ref}}\right)^2\right]}$$

Here, μ_n^{LI} considers ionized impurity scattering, μ_n^{LIS} adds surface scattering, and μ_n^{LISF} gives the final mobility including velocity saturation. The depth dependence model uses y^{ref} as a parameter. Since the model is phenomenological, the parameters for surface scattering and velocity saturation may depend on the fabrication process. To yield physically meaningful results, valid for a large range of gate lengths, appropriate devices and bias conditions must be selected during the calibration. After disabling the high-field mobility degradation term, the error in the maximum drain current of the 4 μm device was found to be about 2%. Hence, it was decided to calibrate the surface mobility parameters using this long-channel device. With these values, the calibration of the high-field mobility parameters was carried out with the short-channel device, where a strong high-field degradation could be expected.

2. The VISTA Framework

The calibration was automatically run using our VISTA framework [1] with fifteen operating points selected from the measured IV-curves. VISTA supports a rigorous job farming algorithm which allows the efficient usage of all hosts available in the cluster. Since there were 21 hosts available, optimization could be speed up significantly resulting in a total of about two hours for the optimization of the surface scattering parameters and even less then one hour for the optimization of the velocity saturation parameters.

3. Actual Calibration

Before performing any calibrations on the 4 μm device, the simulation results obtained by using the default mobility parameters were compared with measurements. To ac-

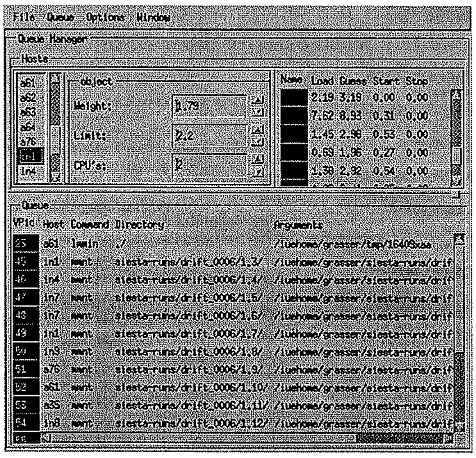

Figure 1. VISTA Framework showing load information.

count for the unknown interface charges, the work function difference was adjusted to $E_w = -0.6$ eV to reproduce a current of $I_d(V_{th}) = 10$ nA for the measured threshold voltage of $V_{th} = 0.15$ V (device width is 15 μm). This approximation is valid under the assumption that the influence of the surface and high-field mobility parameters on the drain current are negligible under these bias conditions. As expected, the comparison showd good agreement for the sub-threshold region, whereas the drain current for maximum bias was overestimated by 17%.

3.1. Surface Mobility Parameters

As a first step, the three surface mobility parameters μ_n^{ref}, y^{ref}, and γ_n for the 4 μm device where calibrated. Using the optimized parameters for the simulation, the resulting maximum absolute error in the drain current was found to be less than 2.3% in the entire range.

3.2. High Field Parameters

Before concentrating on the high-field parameters, the optimum parameters extracted with the 4 μm device were tested for their accuracy when used for the 0.25 μm device. As before, only the threshold voltage has been adjusted to satisfy the threshold condition. This adjustment ($E_w = -0.53$ eV) is necessary to compensate for the inaccuracies of the process simulation for deep-submicron devices. The agreement was found to be exceptionally good. For high-bias conditions, the drain current is overestimated by only 2%.

For the optimization of the high-field parameters S_n^{ref}, v_n^{sat}, and β_n, the selected fifteen operating points for the 0.25 μm device were restricted to the high-bias region. With the optimized values the simulation shows a very small error (0.7%) for the higher bias conditions and a maximum error (2.4%) for intermediary bias conditions.

4. Discussion

The optimum found is summarized in Table 1. All parameters show physically sound deviations from their respective default values. In particular it is worthwhile to mention, that the saturation-velocity which is a quite firm quantity in terms of physical reasoning, was just marginally adapted by the automatic optimization procedure. Furthermore it is to note, that the large deviation of −60% in the surface parameter y^{ref} denotes the improvement in process technology compared to typical processes investigated in [5]. Since there are many uncertainties in the exact doping profile, gate length, etc., the calibrated parameters reflect the average variations of these process parameters.

To test the accuracy of these values for devices with even shorter gate lengths, simulations with the 0.2 μm device were carried out. Again, the accuracy is very good considering the large uncertainty of the process data for such small gate lengths. The final results for the cases with $L_g = 4$ μm and $L_g = 0.25$ μm, using the calibrated values are shown in the Fig. 2 – Fig. 3, respectively.

Table 1. Summary of the optimized mobility model parameters.

Par.	Opt.	Def.	[%]	Unit
μ_n^{ref}	538	638	-15.7	cm^2/Vs
y^{ref}	3.96	10	-60	nm
γ_n	1.33	1.69	-21.3	1
S_n^{ref}	5.933e7	7e7	-15.2	V/m
v_n^{sat}	1.48e7	1.45e7	2	cm/s
β_n	2.217	2	10.8	1

[1] C. Pichler, R. Plasun, R. Strasser, and S. Selberherr, "High-Level TCAD Task Representation and Automation," *IEEE Trans.Semiconductor Technology Modeling and Simulation*, May 1997. `http://www.ieee.org/journal/tcad/accepted/pichler-may97/`.

[2] Technology Modeling Associates, Inc., Palo Alto, CA, *TMA TSUPREM-4, Two-Dimensional Process Simulation Program, Version 6.2*, June 1995.

[3] Technology Modeling Associates, Inc., Palo Alto, CA, *TMA MEDICI, Two-Dimensional Device Simulation Program, Version 2.0*, Sept. 1994.

[4] C. Fischer, P. Habaš, O. Heinreichsberger, H. Kosina, P. Lindorfer, P. Pichler, H. Pötzl, C. Sala, A. Schütz, S. Selberherr, M. Stiftinger, and M. Thurner, *MINIMOS 6 User's Guide*. Institut für Mikroelektronik, Technische Universität Wien, Austria, Mar. 1994.

[5] S. Selberherr, W. Hänsch, M. Seavey, and J. Slotboom, "The Evolution of the MINIMOS Mobility Model," *Solid-State Electron.*, vol. 33, no. 11, pp. 1425–1436, 1990.

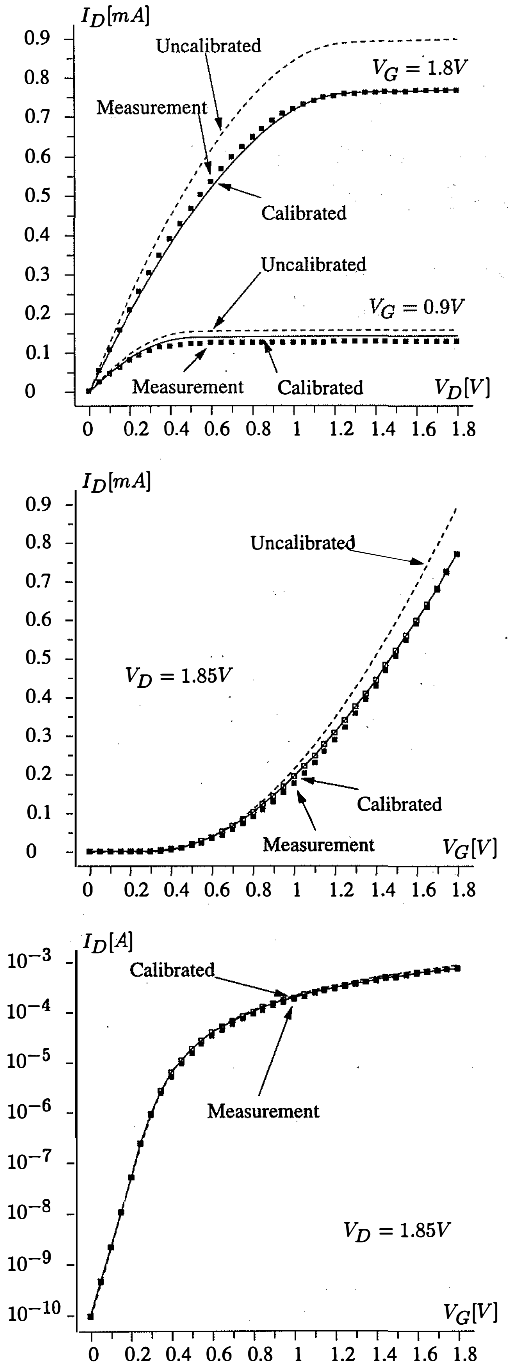

Figure 2. Comparison of simulation and measurement for the $L_g = 4$ μm device.

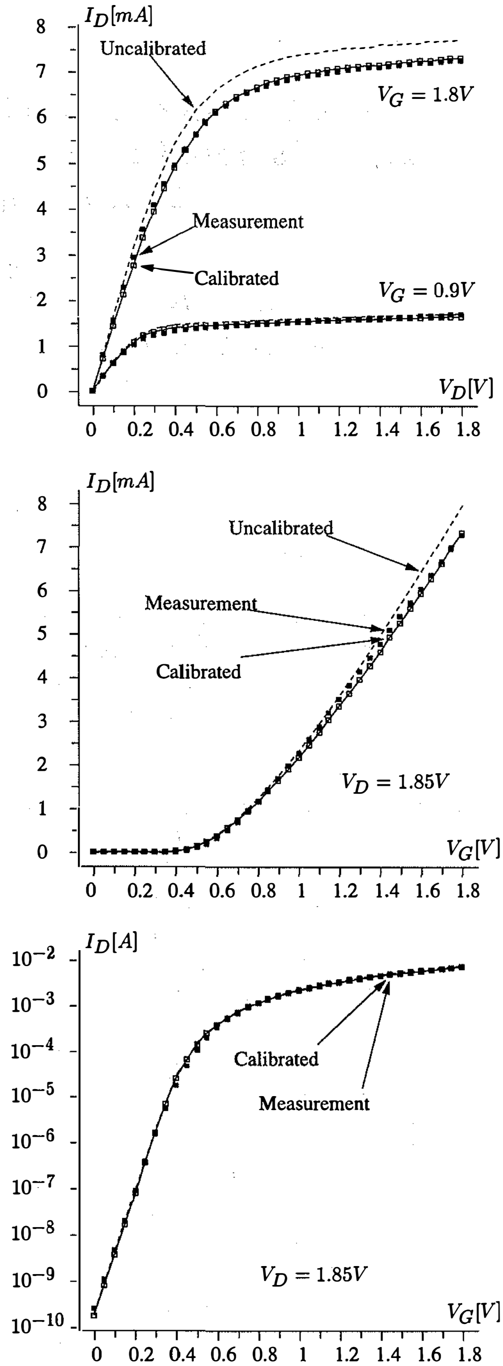

Figure 3. Comparison of simulation and measurement for the $L_g = 0.25$ μm device.